Numerical Simulation of Transient Crack Growth Experiments

T.-J. SHIUE and K. RAVI-CHANDAR
Department of Mechanical Engineering, University of Houston, Houston, Texas 77204–4792, USA

I. Introduction

In this paper transient crack growth under stress wave loading is simulated using a fine grid finite element mesh. The simulations duplicate exactly the loading conditions and crack growth observations reported in [1]. The results of the simulation are used to determine the range of dominance of asymptotic singular field and also examine the experimental methods of photoelasticity and caustics used to determine K_I. Analytical results of Freund [2] and Ma and Freund [3] which also address the same problems as the experiments in [1] and the present numerical simulations are also used for comparison. In the following, we briefly outline the crack problem and the finite element simulation of crack growth in Section II. The numerical simulation of the method of caustic is discussed in Section III. Finally in Section IV, dynamic photoelasticity is simulated from the numerical results.

II. Transient Crack Growth Problem

A pressurized semi-infinite crack in an infinite plane elastic medium is considered. This problem is governed by the equation of motion:

$$\sigma_{\alpha\beta,\beta} = \rho\, \ddot{u}_\alpha \quad \text{in } \Omega \tag{1}$$

(α, β have the range 2 and summation convention is used) with boundary conditions:

$$\sigma_{22}(\mathbf{x},t) = -\sigma_0 f(t) \quad \text{on } x_2 = 0,\ x_1 < 0 \tag{2}$$

$$\sigma_{12}(\mathbf{x},t) = 0 \quad \text{on } x_2 = 0,\ x_1 < 0$$

The crack is stationary for $t < \tau$. At $t = \tau$, the crack begins to grow along the line $x_2 = 0$ at a constant speed v. This problem was treated analytically by Freund [2] who gave the variation of stress intensity factor K_I as shown in [3]. Experimental simulation of the same problem was successfully demonstrated in [1]. However, for running cracks, it was found that under certain conditions, the dynamic K-field did not dominate the stress field over a significant distance from the crack tip, particularly where measurements of K_I were

attempted using the method of caustics or photoelasticity [3,4]. In the present work, the above transient crack growth problem is modeled by a very fine mesh finite element scheme, illustrated in Fig. 1. After space discretization, (1) becomes

$$\underline{M}\,\bar{\ddot{d}} + \underline{K}\,\bar{d} = \bar{F} \quad \text{in} \quad \Omega \tag{3}$$

where $\underline{M}$ is the mass matrix, $\underline{K}$ is the stiffness matrix, F is the force vector and d is the displacement vector. Discretization of time domain using alpha method yields

$$\underline{M}\,\bar{a}_{n+1} + (1+\alpha)\,\underline{K}\,\bar{d}_{n+1} - \alpha\,\underline{K}\,\bar{d}_n = \bar{F}(t_{n+\alpha})$$

where $t_{n+\alpha} = (1+\alpha)\,t_{n+1} - \alpha t_n = t_{n+1} + \alpha\Delta t$

$$\bar{d}_{n+1} = \bar{d}_n + \Delta t\bar{v}_n + \frac{\Delta t^2}{2}[(1-2\beta)\,\bar{a}_n + 2\beta\bar{a}_{n+1}] \tag{4}$$

The formulation given above is cited from [5]; the program DLEARN in the last chapter of that book is used in our study. As implemented, DLEARN cannot be used to solve the dynamic crack growth problem mainly because the size of system of equations is fixed. To solve the current problem, we implemented a moving mesh procedure and node releasing technique into DLEARN by the following steps.

Step 1. Although the degrees of freedom in x_2 direction of the nodes on prospective crack line ($x_2 = 0$, $x_1 > 0$) are fixed before crack tip reaches the nodes, they are treated as free when we allocate space for system of equations.

Step 2. After space allocation, the equations reserved for nodes on prospective crack line are deactivated.

Step 3. Moving mesh procedure: Atluri and Nishioka proposed a moving singular element to simulate dynamic crack growth [6]; here, we implement the moving mesh concept using four node isoparametric element. This procedure is illustrated in Figure 2. In Figure 2(ii), when the crack has moved a small distance Δs, the x_1 coordinate and data (displacement, velocity, and acceleration vectors) of node a and it's neighboring nodes are obtained by interpolation. The mass and stiffness matrices of elements 1, 2, 3, 4, 5, 8 also have to be reevaluated. The above process is repeated until the aspect ratio of element 8 is too small; then switching is needed so that the crack can run further. the switching is completed by discarding the data of nodes e, h, then moving the data of d, g, to e, h respectively (also c, a to d, g and b, f, to c, a), then storing data of i, j obtained by interpolation to b, f.

Step 4. In Fig. 2(iv), crack tip has run over node f, so the degree of freedom in the x_2 direction of node f must be released; this is equivalent to adding another equation to the system of equations by using the space reserved in step 1.

III. Numerical Simulation of the Shadow Optical Method of Caustics

In the thesis [1] by K. Ravi-Chandar, a transparent material Homolite-100 was used in the experiment and the dynamic stress intensity factor was determine by the shadowoptics method of caustics. Breifly, shadowoptics may be described as follows: let a family of light rays fall perpendicularly on specimen near the crack tip. Due to the thickness variation of the specimen and stress-optic effect there is a shadow spot on the reference plane which is

placed a distance Z_0 from the specimen. In [1] the size of the shadow spot was recorded by a camera about every 10 μsec; K_I is then calculated from the size of the shadow spot by the formula

$$K_I = \frac{2}{3}\frac{\sqrt{2\pi}}{Z_0 ch}\left(\frac{D}{f_c}\right)^{5/2} F(v) \tag{5}$$

where c is the stress optic constant, h is the undeformed thickness, D is the transverse diameter of the shadow spot, $f_c = 3.17$, F(v) is a function of crack speed given in [7].

We simulate the experiment numerically by using the shadow optical mapping equations relating the screen coordinate to stress field:

$$X_\alpha = x_\alpha - Z_0\frac{\partial f_1}{\partial x_\alpha} \quad , \quad \alpha = 1,2$$

$$f_1(x_1,x_2) = ch\,(\sigma_1 + \sigma_2) \tag{6}$$

where X_α is a coordinate system on the screen, x_α is one on the specimen, and σ_1, σ_2 are the principal stresses. Figure 3 shows one shadow spot plot from the numerical simulation. For each such plot, transverse diameter of shadow spot is measured and formula (5) is used to calculate K_I; thus time history of K_I by numerical simulation can be obtained as shown in Figure 5. The size of the shadow spot depends on Z_0 and in the simulation, Z_0 was held constant at the value used in [1].

IV. Numerical Simulation of Dynamic Photoelasticity

Another common experimental method for the determination of the stress intensity factor is dynamic photoelasticity. A review of this technique applied to dynamic crack growth is given in [8]. For the case of a stationary crack, the isochromatic fringe loops are described by:

$$\left(\frac{Nf_o}{h}\right)^2 = \frac{K_I^2}{2\pi r}\sin^2\theta + \sqrt{\frac{2}{\pi r}}\,K_I\,\sigma_{ox}\sin\frac{\theta}{2}\,\sin\theta\,(1+2\cos\theta) + \sigma_{ox}^2 \tag{7}$$

where f_o is the stress-fringe value, h is the plate thickness and σ_{ox} is the first non-singular order term in the expansion for σ_{11}. In dynamic photoelastic experiments, the isochromatics are photographed and then (7) is used to obtain K_I and σ_{ox}. A similar equation can be developed for the case of a rapidly growing crack.

The results of the numerical simulation were used to examine the method of photoelasticity. From the numerical results, isochromatic fringes (contours of constant $\sigma_1 - \sigma_2$) were obtained. This is shown in Figure 4. Then, from the simulated isochromatics, the fringe data (N, r, θ) were obtained at several fixed radii. These were then used in (7) through the over determined least square curve fit technique to obtain K_I and σ_{ox}; it should be pointed out that the numerical results do not show a dominance of the K-field as determined by the variation of σ_{22} along $\theta = 0$ over the region over which the isochromatic data were obtained and thus using (7) implies that we are forcing a K-field. The results of this procedure is shown in Figure 6 for the same two cases as in Figure 5.

Results from the four different approaches-theoretical, experimental, numerical caustic simulation, and numerical photoelastic simulation are compared for two different crack growth cases. K_I from all the methods agree very well before the crack starts running.

After that the experimental K_I grows continuously, the analytical one shows a drop followed by a slight increase. The numerical results show oscillations that are probably due to the discrete nature of the nodal release procedure. This aspect is under further investigation.

References

1. K. Ravi-Chandar, "An Experimental Investigation into the Mechanics of Dynamic Fracture," Ph.D. Thesis, California Institute of Technology, June 1982.

2. L.B. Freund, *Journal of the Mechanics and Physics of Solids*, **21**, (1973), pp. 47.

3. C.C. Ma, and L. B. Freund, *Journal of Applied Mechanics*, **53**, (1986), pp. 303-310.

4. K. Ravi-Chandar and W. G. Knauss, *Journal of Applied Mechanics*, **54**, (1987), pp. 72-78.

5. T. J. R. Hughes, "The Finite Element Method," Englewood Cliffs, N.J., Prentice-Hall, (1987), pp. 532.

6. S. N. Atluri, T. Nishioka and M. Nakagaki, *Nonlinear and Dynamic Fracture Mechanics*, ASME AMD 35, editors: N. Perone and S. N. Atluri, (1979), pp. 37-67.

7. C. C. Ma, "An Examination of Crack Tip Fields in Brittle Materials Subjected to Dynamic Loading," Ph.D. Thesis, Brown University, May 1985.

8. J. W. Dally, *Experimental Mechanics*, **19**, (1979), pp. 349-361.

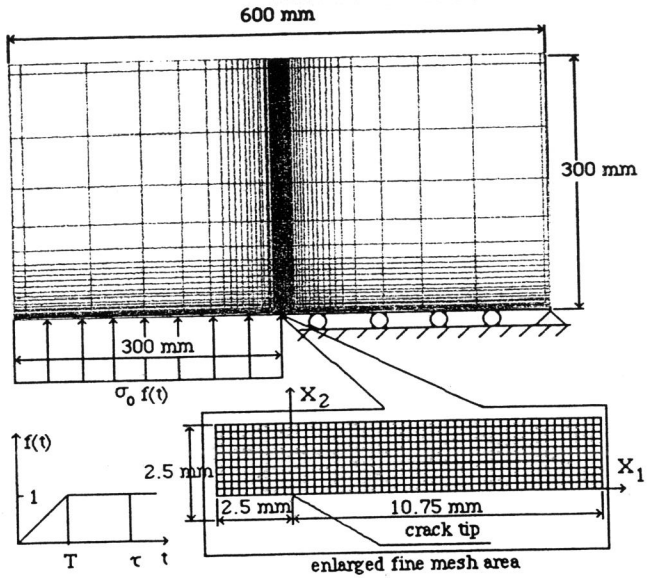

Fig 1. Finite element mesh for dynamic crack growth problem

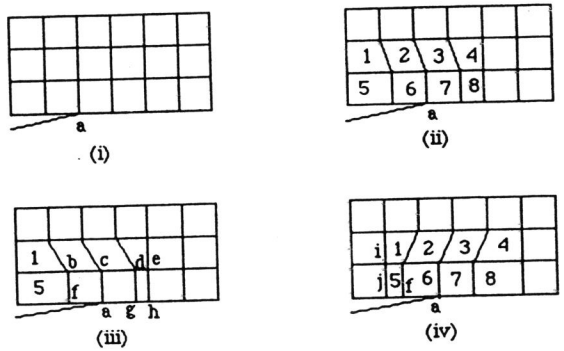

Fig 2. Moving mesh scheme for dynamic crack growth

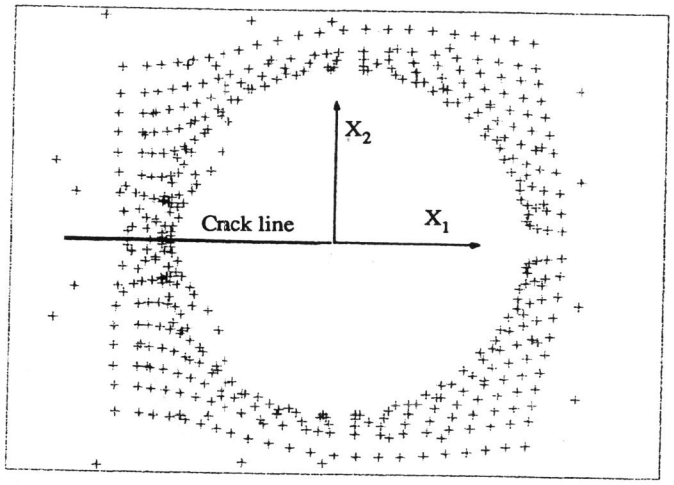

Fig 3. Numerically generated shadow spot.

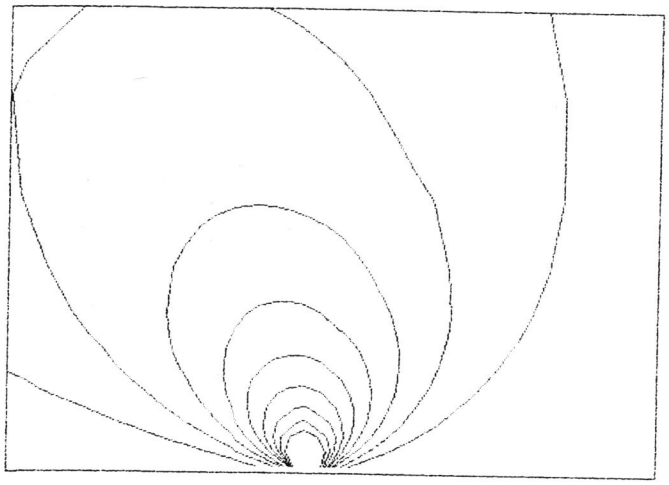

Fig 4. Numerically simulated isochromatic finges

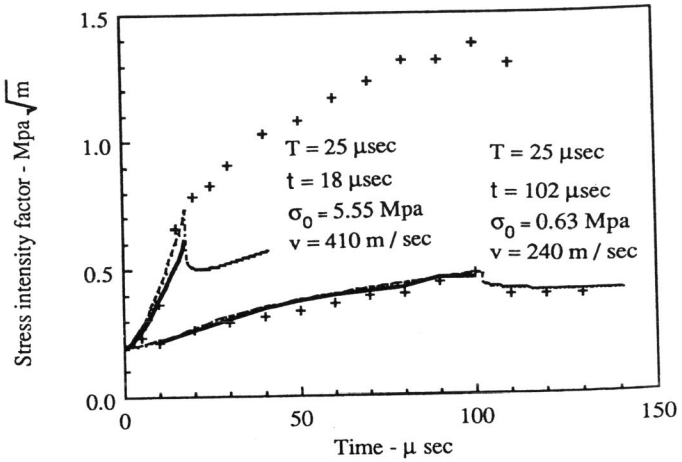

Fig 5. Stress intensity factor histories
(+ experiment,___FEM, --- theory)

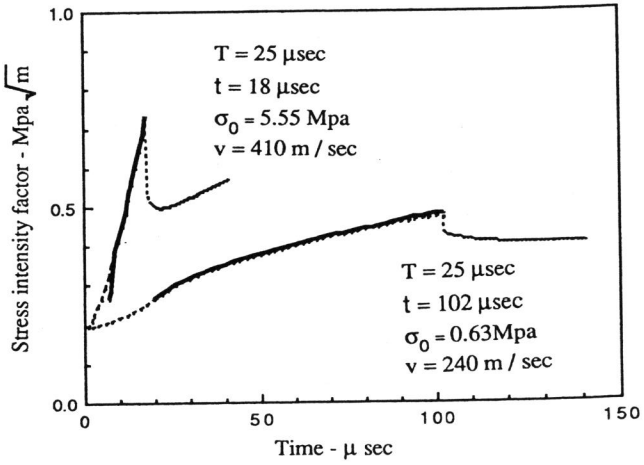

Fig 6. Stress intensity factor histories
(--- theory, ___ Photoelasticity)